

EXPERIMENTAL STUDY OF HALO FORMATION AT ATF2 *

R. Yang[†], P. Bambade, S. Wallon, V. Kubytskyi, LAL, Orsay, France
 A. Faus-Golfe, N. Fuster-Martínez, IFIC, Valencia, Spain
 A. Aryshev, T. Naito, N. Terunuma, KEK and SOKENDAI, Ibaraki, Japan

Abstract

For the Accelerator Test Facility 2 (ATF2) and for other high-intensity accelerators, beam halo is an important factor affecting the machine performance as well as potentially causing component activation. It is imperative to clearly understand the mechanisms that lead to halo formation and to test the available theoretical models with an adequate experimental setup. In this paper, measurements of beam halo at ATF2 are presented, which clearly show the influence of the beam gas scattering formation process in the ATF ring. The upgrade of an OTR/YAG screen monitor for more comprehensive halo studies are also introduced.

INTRODUCTION

ATF2 is an extension of the extraction line of Accelerator Test Facility (ATF) at KEK with an ILC-type final focus system [1, 2]. The ATF2 facility was built to demonstrate the feasibility of focusing the beam to 37 nanometers at the virtual interaction point (IP), with nanometer level stability. The background induced in the *Shintake* monitor [3] measuring the small IP beam size by halo particles lost upstream is important to understand and control. This motivates the present work on predicting and measuring the transmission of halo in ATF2 [4–6].

There is no rigorous definition of halo, but one thing is certainly clear, halo is low density and at large radii from a more intense Gaussian beam core [7]. Several theories have been developed [8, 9] to illustrate the mechanisms of halo production and its dynamics at ATF. These studies show that Beam-Gas Scattering (BGS), Intra-Beam Scattering (IBS) and misalignments of magnets might induce halo. However, experimental studies have not so far enabled to fully characterize the origin of the beam halo through detailed comparisons with theoretical calculations and simulations.

Experimental studies of beam halo are difficult because of the high dynamic range, larger than 10^5 , typically required to meaningfully measure the distribution. In order to achieve efficient halo visualization, several instruments have been developed and installed at ATF2, e.g. wire scanners (WS), diamond sensors (DS) and a YAG:Ce screen. In this paper, we report the results of detailed halo measurements using the DS, which show that the vertical beam halo is dominated by BGS at ATF. Motivations and plans for upgrading the YAG monitor are also described.

PREDICTION OF BEAM HALO AT ATF2

The BGS mechanism has been considered as one of the main mechanisms for halo formation and analytical methods were developed to estimate the resulting distortion of beam distribution [8, 9], treating the stochastic scattering incoherently as a slow diffusion process. To valid the analytic approximation, a systematic simulation has been performed [10], which successfully achieves a good agreement with the theoretical predictions, as shown in Fig.1. In addition, the vacuum dependence of the beam halo formation is predicted for typical gas pressures. The SAD tracking program [11] is used to propagate the halo to the diagnostic devices located along ATF2.

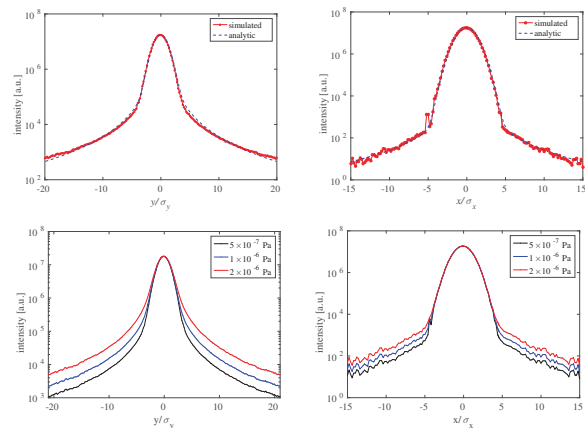


Figure 1: (Upper) Comparison of non-Gaussian beam profiles evaluated theoretically and by simulation; (Bottom) Evolution of beam halo with various vacuum pressure.

MEASUREMENT OF BEAM HALO

Experimental Technique

To measure the transverse beam halo with a satisfactory dynamic range, an in vacuum diamond sensor detector has been built [12]. The DS detector consists of a single crystal vapor deposition (sCVD) diamond of 500 μm thickness, metalized with two broad strips of 1.5 mm \times 4 mm and two narrow strips of 0.1 mm \times 4 mm. The strips and related circuitry are mounted on a ceramic PCB suitable for ultra-high vacuum, as shown in Fig.2. A -400 V bias voltage is used and the collected ionization charge is measured on a 50 Ω resistor. The dynamic range measured with beam can reach 10^4 , with a lower limit of 10^3 electrons, due to pick up noise, and a linear response up to $\sim 2 \times 10^7$ electrons, limited by charge collection saturation effects in the diamond [13].

* Work supported by Chinese Scholarship Council

[†] ryang@lal.in2p3.fr

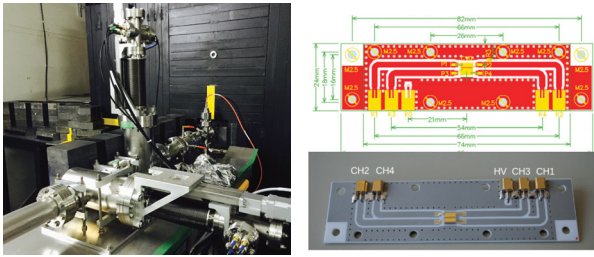


Figure 2: (Left) Horizontal and vertical DS detectors at Post-IP; (Right) Layout of the diamond strips (centered with golden color) on the PCB.

For the typical ATF2 beam intensities and optics [2], the number of electrons hitting the broad DS strips ranges from 10^3 to more than 10^8 . The beam core distribution is distorted because of the nonlinear response of the DS for high carrier density, as shown in Fig.3. To mitigate the decrease of charge collection efficiency (CCE) due to the nonlinear response, a number of strategies have been suggested, for instance, adding a $1\ \Omega$ resistor in parallel to the readout resistor to reduce the voltage drop, or else relying on rescaling of beam profile based on separate calibrations, or predicting the distortion from the saturation using a theoretical model [12, 14].

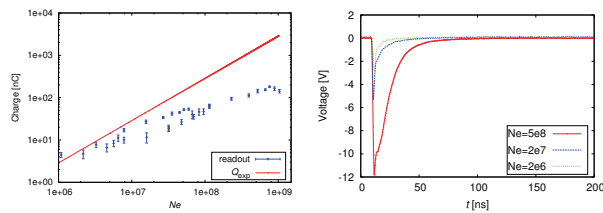


Figure 3: (Left) Charge signal as a function of the quantity of electrons collected ; (Right) Typical waveforms when DS is in the core region.

In this paper, a self-calibration method is applied to the beam core to mitigate the saturation effect. It consists in assuming a Gaussian beam core distribution measured by the WS located 2.89 m upstream and propagating it to the DS to predict the number of electrons striking each of its strips according to position with respect to the beam center. Subsequently, the charge collection Q_{exp} which could be expected in the absence of saturation is computed based on the known CCE measured at low incident charge. The rescaling factor κ is then defined by the ratio of Q_{exp} and charge signal readout, and applied to rescale the distribution. In this way, the dynamic range can be extended beyond 10^5 with a linear response in the range $1 \times 10^3 \sim 5 \times 10^8$ electrons. The beam profile resulting from this rescaling process is comparable with the prediction, as shown in Fig.4.

Experiment Studies with DS Detectors

To study the generation of beam halo due to BGS in the ATF damping ring, the beam core and halo were mea-

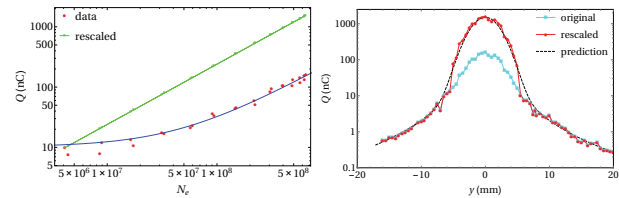


Figure 4: Estimation of rescaling factor based on self-calibration (left) and beam profile after rescaling (right).

sured for various vacuum levels. The beam intensity was 3×10^9 /pulse, and the gas pressure was adjusted by turning on/off part of the ions pumps in the arc sections. After implementing the rescaling approach, satisfactory agreement between the vertical profiles measured and simulated could be achieved for the different vacuum levels. An increase in beam halo for the degraded vacuum conditions is also clearly observed, as shown in Fig.5. Based on the good consistency between the analytical approximation, simulation and measurement results, we could conclude that the main source of vertical beam halo at ATF2 is beam gas Coulomb scattering in the damping ring.

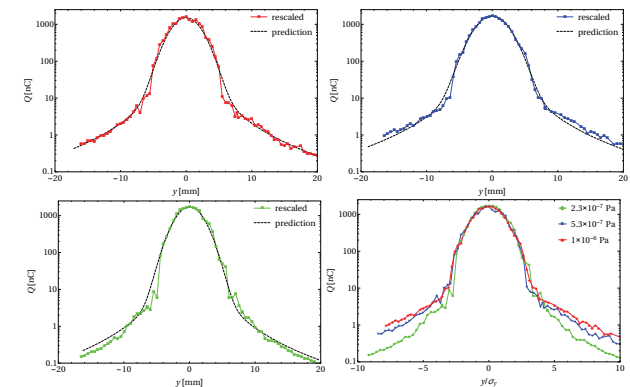


Figure 5: Reconstructed vertical beam profiles for typical vacuums.

The measured horizontal beam distributions were also corrected for saturation effect using the described self-calibration method. The reconstructed beam profiles do approach the predictions from BGS, but an asymmetry is observed, with more halo on the high energy side, as shown in Fig.6. The evolution of beam halo with the vacuum level was however found to be negligible, which might be due to insufficient sensitivity, since the halo levels are typically two orders of magnitude lower in the horizontal plane. The DS being located in the high dispersion region after a large horizontal bending magnet ($\eta_x \approx 1$ m), potential non-Gaussian tails in the energy distribution of the beam may also have an impact.

Upgrading of An OTR/YAG Screen Monitor

To complement the measurements with the DS, an improved YAG screen monitor combined with an OTR was proposed and fabricated recently. The old monitor uses a

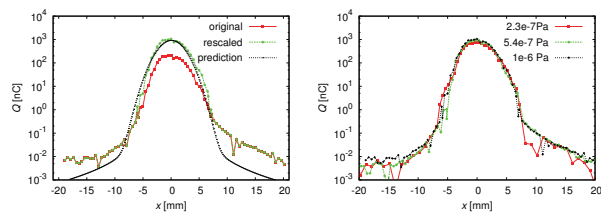


Figure 6: Horizontal beam distribution and its vacuum dependence.

YAG: Ce screen with a 1 mm slit in the center to allow the beam core to pass while the halo hits the screen. The saturation level of the YAG: Ce screen is measured as $0.25 \text{ pC}/\mu\text{m}^2$, which limits the dynamic range to 10^3 [4]. To reduce the systematics in the imaging of beam core and halo, an OTR screen is now also used in addition to several YAG:Ce slices, with slits of $1 \text{ mm} \times 4 \text{ mm}$ in the center, mounted on a common actuator, as shown in Fig.7. Two horizontal YAG: Ce slices are cut by 45 degree to avoid the edge effect. The screens are inserted into the beam orbit at 45 degree in the horizontal direction. The OTR screen is oriented at 22.5 degree to collect the OTR and scintillation light using the same high sensitivity CCD camera from the perpendicular direction, with an expected dynamic range of 10^5 . The new OTR/YAG screen monitor will be installed in a dispersion free region, which will enable separating betatron and energy halo, as well as measuring the possible momentum diffusion.

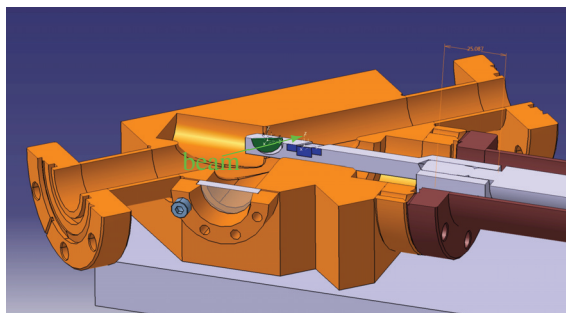


Figure 7: Configuration of the OTR/YAG screen monitor.

To minimize the wakefield impact on the ultra-small vertical beam size at ATF2, the mechanical design of the chamber and holder was optimized carefully. A realistic numerical simulation of wakefields was performed with CST PS [15]. The amplitude of the vertical wake potential was shown to be less than 0.05 V/pC for vertical displacement of 5 mm, inducing an orbit distortion of less than 0.9 nm and a RMS beam size growth of 0.5 nm at the IP, as shown in Fig.8.

CONCLUSION

Experimental studies of beam halo generation at ATF2 have been performed with a diamond sensor detector. To suppress the decrease of the CCE for beam core scanning, an approach to rescale the beam distribution has been developed and applied successfully. Satisfactory agreement between

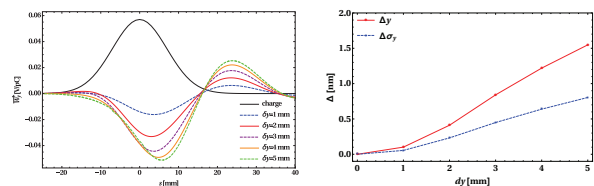


Figure 8: Wake potential (left) and its impact on beam at the IP.

theoretical predictions and measurements has been obtained, and a clear enhancement of the vertical beam halo for the worsened vacuum conditions was observed. This indicates that the vertical beam halo at ATF2 is mainly determined by BGS in the damping ring. However, the evolution of the horizontal beam halo as a function of vacuum level is not evident. The asymmetric horizontal beam distribution implies the existence of other halo sources, which might be IBS, wakefields or other effects. To visualize beam halo in a dispersion free region, an improved OTR/YAG screen monitor has been designed and manufactured. A dynamic range of 10^5 is expected with a high quality CCD camera. Numerical simulation suggests negligible influences from wakefield effects. Performance tests of this monitor will be done in the coming beam operation.

ACKNOWLEDGMENT

We thank N. Delerue, K. Kubo and T. Okugi for helpful discussions, comments and commissioning assistance.

REFERENCES

- [1] Grishanov *et al.*, "ATF2 proposal", 2005, <https://arxiv.org/pdf/physics/0606194.pdf>
- [2] G. White *et al.*, "Experimental validation of a novel compact focusing scheme for future energy-frontier linear lepton colliders", *Phys. Rev. Lett.* 112, 034802, 2014.
- [3] S. Taikan, *et al.*, "A nanometer beam size monitor for ATF2", *Nucl. Inst. Meth.*, 616D(1), 2010.
- [4] T. Naito and T. Mitsuhashi, "Beam halo measurement utilizing YAG:Ce screen", in *Proc. IBIC'15*, Melbourne, Australia, September 2015, pp. 373-376.
- [5] R. Yang, *et al.*, "Modeling and experimental studies of beam halo at ATF2", in *Proc. IPAC'16*, Busan, Korea, May 2016, p88.
- [6] N. Fuster-Martínez, *et al.*, "Performance Studies of a Single Vertical Beam Halo Collimation System at ATF2", in *Proc. IBIC'16*, Barcelona, Spain, September 2016, pp. 139-142.
- [7] H. Zhang, *et al.*, "Beam halo imaging with a digital optical mask", *PRST-AB* 15, 072803, 2012.
- [8] H. Kohji and K. Yokoya, "Non-Gaussian distribution of electron beams due to incoherent stochastic processes", KEK, 1992.
- [9] T. Raubenheimer, "Emittance growth due to beam-gas scattering", KEK, 1992.

- [10] R. Yang, *et al.*, “Numerical investigation of beam halo formation from beam gas scattering in KEK-ATF”, presented at IPAC’17, Copenhagen, Denmark, May 2017, paper MOPAB029, this conference.
- [11] SAD is a computer program for accelerator design. <http://acc-physics.kek.jp/SAD/sad.html>
- [12] S. Liu, *et al.*, “In vacuum diamond sensor scanner for beam halo measurements in the beam line at the KEK Accelerator Test Facility”, *Nucl. Inst. Meth.* A832, 2016.
- [13] A. Many, “Theory of transient space-charge-limited currents in solids in the presence of trapping”, *Phys. Rev.* 126 (6), 1962.
- [14] V. Kubytskyi, *et al.*, “Modeling/measurement comparison of signal collection in diamond sensors in extreme conditions”, in *Proc. IPAC’16*, Richmond, USA, May 2015, MOPHA007.
- [15] <https://www.cst.com/products/cstps>